0273-2289/1559-0291 (Online)/07/136/0077/$30.00

Preparation of Chitosan Nanoparticles as Carrier for Immobilized Enzyme

Zhen-Xing Tang,*[,1] Jun-Qing Qian,[2] and Lu-E Shi[1]

[1]College of Chemical Engineering and Materials Science and [2]College of Pharmaceutical Science, Zhejiang University of Technology, Hangzhou 310014 Zhejiang China, E-mail: tangzhenxing@126.com

Received February 6, 2006; Revised February 21, 2006; Accepted February 27, 2006

Abstract

This work investigated the preparation of chitosan nanoparticles used as carriers for immobilized enzyme. The morphologic characterization of chitosan nanoparticles was evaluated by scanning electron microscope. The various preparation methods of chitosan nanoparticles were discussed and chosen. The effect of factors such as molecular weight of chitosan, chitosan concentration, TPP concentration, and solution pH on the size of chitosan nanoparticles was studied. Based on these results, response surface methodology was employed. The results showed that solution pH, TPP concentration, and chitosan concentration significantly affected the size of chitosan nanoparticles. The adequacy of the predictive model equation for predicting the magnitude orders of the size of chitosan nanoparticles was verified effectively by the validation data. Immobilization conditions were investigated as well. The minimum particles size was about 42 ± 5 nm under the optimized conditions. The optimal conditions of immobilization were as follows: one milligram of neutral proteinase was immobilized on chitosan nanoparticles for about 15 min at 40°C. Under the optimized conditions, the enzyme activity yield was 84.3%.

Index Entries: Chitosan; nanoparticles; immobilization; response surface methodology.

Introduction

Chitosan, poly [β-(1-4)-linked-2-amino-2-deoxy-D-glucose], is the *N*-deacetylated product of chitin, which is a major component of arthropod and crustacean shells such as lobsters, crabs, shrimps, and cuttlefishes

*Author to whom all correspondence and reprint requests should be addressed.

(1). The difference between chitosan and chitin is only in the functional group situated at carbon-2 of the monomeric unit. Owing to the presence of free amine groups in chitosan, the solubility and reactivity of this polymer are greater than those of chitin *(2)*. In addition, chitosan has many significant biologic and chemical properties: it is biodegradable, biocompatible, bioactive, and polycationic *(3)*. Thus, it has been widely used in many industrial and biomedical aspects, including in wastewater treatment, as chromatographic support, in enzyme immobilization, and as carrier for controlled drug delivery *(4–7)*. In addition, chitosan is economically attractive because chitin is the most abundant natural polymer after cellulose. However, chitosan is macromolecular, which significantly affects its application. To overcome this drawback, the use of chitosan-fabricated nano/submicron chitosan is effective.

In recent years, nanotechnology has showed significant attractiveness for the preparation of immobilized enzyme carriers. Under the scale of nano, nanomaterials have characteristics such as magnetism and large surface area. These characteristics are favorable for enzyme immobilization. Many studies have mainly reported the preparation of chitosan nanoparticles and their applications in the carrier of drugs *(8–17)*, but few studies have reported the applications in enzyme immobilization.

To the best of our knowledge, studies of neutral proteinase immobilized on chitosan nanoparticles have rarely been reported. In the present study, we discussed and chose the preparation methods of chitosan nanoparticles. In addition, we analyzed factors that influenced the size of chitosan nanoparticles, and employed response surface methodology (RSM) to optimize their size. Furthermore, we immobilized neutral proteinase on chitosan nanoparticles and studied the conditions for immobilization. All the results provide a sound basis for further exploration.

Materials and Methods

Enzymes and Chemicals

Neutral proteinase (2000 U/mg), a commercial enzyme of food-grade preparation, was obtained from Wuxi Enzyme Preparation Factory (Jiangshu, China). Chitosan with different degrees of deacetylation and different molecular weights was provided by Yuhuan Ocean Biochemical (Zhejiang, China). Sodium polyphosphate (TPP) was purchased from Dongsheng Chemical Preparation Factory (Zhejiang, China). All other chemicals were of analytical grade and no further purification was required.

Choice of Preparation Methods for Chitosan Nanoparticles

Preparation of Chitosan Nanoparticles in Nonwater Phase

One percent chitosan solution was prepared using 2.0% aqueous acetic acid solution. Then it was poured dropwise into dispersion medium composed of mineral oil, petroleum ether, and emulsifier. During this pro-

cess, the dispersion medium was stirred at 1000–2000 rpm for 10 min at room temperature. At the end of this period, chitosan nanoparticles were washed consecutively with petroleum ether, acetone, and water. The nanoparticles were further investigated for SEM and application.

Preparation of Chitosan Nanoparticles in Water Phase

Chitosan nanoparticles were prepared based on ionic gelation method. Various concentrations of chitosan (0.10, 0.30, 0.50, 0.80, 1.0, 1.5, and 2.0%) were dissolved in acetic aqueous solution. At room temperature, 20 mL of various concentrations of TPP solution (0.25, 0.50, 0.75, 1.0, 1.25, 1.5, and 2.0 mg/mL) were added to 40 mL of chitosan solution, respectively. Three types of phenomena were observed: solution, aggregates, and opalescent suspersion. The zone of opalescent suspension was further examined as nanoparticles.

Experimental Design and Data Analysis

The purpose of the first optimization step was to determine which factors had a significant effect on the size of chitosan nanoparticles. Five factors—molecular weight of chitosan, chitosan concentration, solution pH, stirring rate, and temperature—were studied using a 2^{5-2} fractional factorial design (FFD) involving two concentrations of each factor *(18)*. Experiments were carried out at the center of the design as internal standards to find the accuracy of the results of statistical experimentation. Table 1 gives the experimental design of the first optimization step. The actual concentration of each factor was coded according to Eq. 1 to facilitate multiple regression analysis:

$$X_i = (x_i - x_0)/\Delta x_i \tag{1}$$

in which X_i is the independent variable coded value, x_i is the independent variable real value, x_0 is the independent variable real value on the center point, and Δx_i is the step change value.

The experimental data obtained from the FFD was then fitted to the following first-order regression model, which could be used to screen important variables and construct the steepest ascent path. The variable with the larger coefficient had a more significant effect on the response compared with the small one, and the positive or negative effect of the variable on the response could be determined by the sign of the coefficient:

$$Y = c_0 + \sum_{i=1}^{5} a_i X_i \tag{2}$$

in which Y is the predicted response (the size of chitosan nanoparticles), c_0 is the intercept term and the remaining term, the parameters a_i are the fitted constants for X_i, and the parameters X_i are the coded variables for the tested factors.

If the fitted first-order model is adequate, a series of single experiments must be performed along with the path of steepest ascent toward the

Table 1
Levels of Variables Tested in FFD

Factor	Symbol	Coded level –1	Coded level 1
Chitosan concentration (%)	X_1	0.80	1.2
TPP concentration (mg/L)	X_2	0.25	0.375
Solution pH	X_3	6.0	6.8
Stirring rate (rpm)	X_4	200	300
Temperature (°C)	X_5	30	40

Table 2
Levels of Variables Tested in 2^3 CCD ($\alpha = 1.682$)

Factor	Symbol	Coded level –1	Coded level 0	Coded level 1
Chitosan concentration (%)	X_1	0.80	1.0	1.2
TPP concentration (mg/L)	X_2	0.25	0.325	0.4
Solution pH	X_3	6.2	6.5	6.8

optimum region. From here, the new region of the central point can be detected in which the desirable values of the response are suspected to be within the boundaries of the operability region. Finally, a 2^3 factorial central composite design (CCD) ($\alpha = 1.682$) with nine central points, leading to a total of 23 sets, was used to describe the nature of the response surface in the optimum region. Table 2 gives the levels of each factor. For each of the experiments, the size of chitosan nanoparticles was determined. The response function used was a quadratic polynomial equation as given here:

$$Y = c_0 + \sum_{i=1}^{3} a_{\mathrm{i}} X_{\mathrm{i}} + \sum_{j \le i}^{3} a_{\mathrm{ij}} X_i X_j + \in^{l} \tag{3}$$

in which Y is the predicted response (the size of chitosan nanoparticles), c_0 is the intercept term and the remaining term, the parameters a_i are the fitted constants for X_i, b_{ij} values are the quadratic coefficient, and X_i and X_j are the coded levels of the independent variables.

Experiments were performed in duplicate in shake flasks unless otherwise stated. The data were analyzed using Minitab release 14.0 software. Response surface plots were generated by DPS software. The statistical significance of the regression coefficient was determined by Student's t-test. The level of significance was given as $p < 0.05$. The second-order model equation was determined by Fischer's test, and the quality of the fit of the polynomial model equation was given by the coefficient of determination, R^2. The optimum concentrations of the variables were calculated from the data obtained using DPS software.

Morphology

The morphologic characterization of chitosan nanoparticles was evaluated using a scanning electron microscope (JSM-5610LV; JEOL, Japan).

Conditions of Immobilization

Effect of Time on Immobilization

Eight milliliters of chitosan nanoparticle solution containing 1.0 mg of dry chitosan in the tube was incubated in a water bath for 30 min. Then 1.0 mL of 1.0 mg/mL neutral proteinase was added to the tube, and the mixture was stirred at different times (5, 10, 15, 20, 30, and 40 min). Neutral proteinase immobilized on chitosan nanoparticles was removed by centrifugation, and the supernatant was collected to calculate the residual amount of neutral protein.

Effect of Temperature on Immobilization

Eight milliliters of chitosan nanoparticle solution containing 1.0 mg of dry chitosan in the tube was incubated in a water bath at different temperatures (30, 35, 40, 45, 50, 55, and 60°C) for 30 min, respectively. Then l.0 mL of 1.0 mg/mL neutral proteinase was added to the tube, and the mixture was stirred at intervals of about 15 min. Neutral proteinase immobilized on chitosan nanoparticles was removed by centrifugation, and the supernatant was collected to calculate the residual amount of neutral protein.

Effect of pH on Immobilization

Eight milliliters of chitosan nanoparticle solution containing 1.0 mg of dry chitosan in the tube was incubated in a water bath at different pH values (4.0, 4.5, 5.0, 5.5, 6.0, 6.5, 7.0) for 30 min, respectively. Then 1.0 mL of 1.0 mg/mL neutral proteinase was added to the tube, and the mixture was stirred at intervals of about 15 min. Neutral proteinase immobilized on chitosan nanoparticles was removed by centrifugation, and the supernatant was collected to calculate the residual amount of neutral protein.

Determination of Protein Concentration

Protein concentration was assayed according to the method of Lowry *(18)* with bovine serum albumin as the standard protein.

Determination of Activity of Free Neutral Proteinase and Immobilized Neutral Proteinase

Five milliliters of 0.60% casein solution was added to the tube prepared for measuring enzyme activity. After incubation for 20 min at 40°C, the reaction of proteolysis was started by the addition of 1.0 mL of neutral proteinase or 1.0 mL of buffer solution containing 1.0 mg of immobilized proteinase. The reaction was allowed to stand for 10 min at the same temperature. During the period of proteolysis, the tube was shaken occasionally. The reaction was stopped by the addition of 2.0 mL of 0.40 mol/L

trichloroacetic acid (TCA). The reaction mixture was filtered. A blank was prepared under the same conditions, but 2.0 mL of 0.40 mol/L TCA was added before the addition of 1.0 mL of neutral proteinase, and the blank was not incubated for 20 min with the sample. One unit of the activity of neutral proteinase was defined as 1.0 mg of tyrosine/min at an optical density of 275 nm.

Results and Discussion

Choice of Preparation Methods for Chitosan Nanoparticles

Reverse micelles are thermodynamically stable liquid mixtures of water, oil, and surfactant. Macroscopically, they are homogeneous and isotropic, structured on a microscopic scale into aqueous and oil microdomains separated by surfactant-rich films. One of the most important aspects of reverse micelle–hosted systems is their dynamic behavior. Nanoparticles prepared by conventional emulsion polymerization methods not only are large (>200 nm), but also have broad size range. Preparation of ultrafine polymeric nanoparticles with narrow size distribution can be achieved using reverse micellar medium *(20)*. Using the reverse-phase method, chitosan nanoparticles could be obtained in our experiment. However, their particle size was so small that they could not be collected through the supercentrifugal effect. Moreover, a plentiful amount of solvent was needed.

The use of complexation between oppositely charged macromolecules to prepare chitosan microspheres has attracted much attention because the process is very simple and mild *(21,22)*. In addition, reversible physical crosslinking by electrostatic interaction, instead of chemical crosslinking, has been applied to avoid the possible toxicity of reagents and other undesirable effects. TPP is a polyanion, which can interact with cationic chitosan by electrostatic forces *(23,24)*. Thus, the process is simple, and the method can be applied widely.

Figure 1 presents scanning electron micrographs of nanoparticles prepared by different methods. The nanoparticles were about 50–80 nm in size. However, in Fig. 1B there is some oil phase, which indicates that the product was washed insufficiently.

Factors Influencing Size of Chitosan Nanoparticles

Effect of Molecular Weight of Chitosan on Size of Chitosn Nanoparticles

Figure 2 shows the influence of the molecular weight of chitosan on the size of nanoparticles. A gradual increase in particle size was noted with an increase in molecular weight. This trend might be explained by the fact that a higher molecular weight chitosan interacted with TPP more efficiently than a lower molecular weight chitosan did. The factor was outweighed by the fact that higher molecular weight chitosan was less soluble, and as a result, an increase in particle diameter or even aggregation might be obtained. These results were the same as the findings of Gan *(25)*.

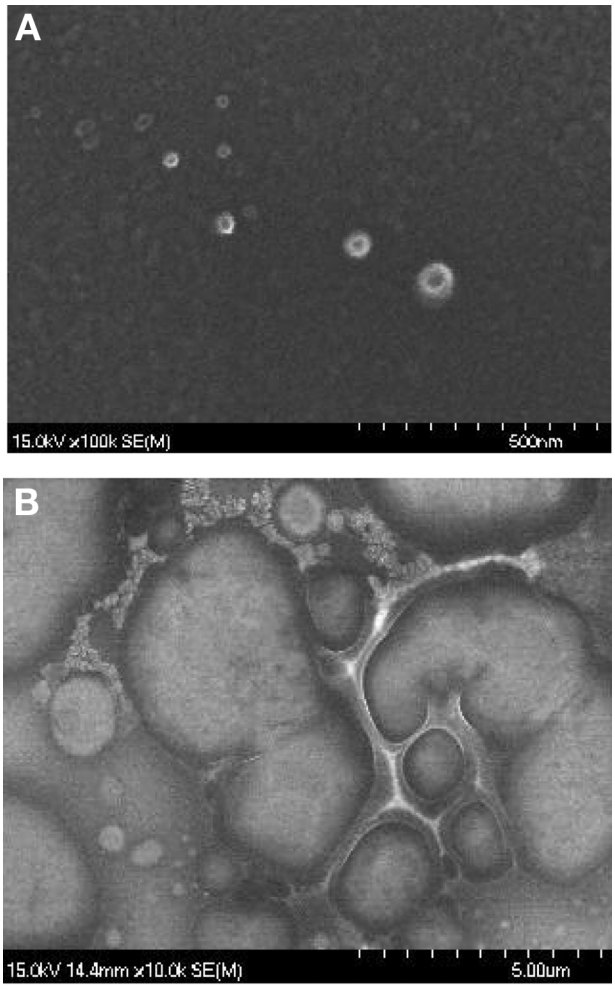

Fig. 1. Scanning electron micrographs of **(A)** nanoparticles made in water phase and **(B)** nanoparticles made in nonwater phase.

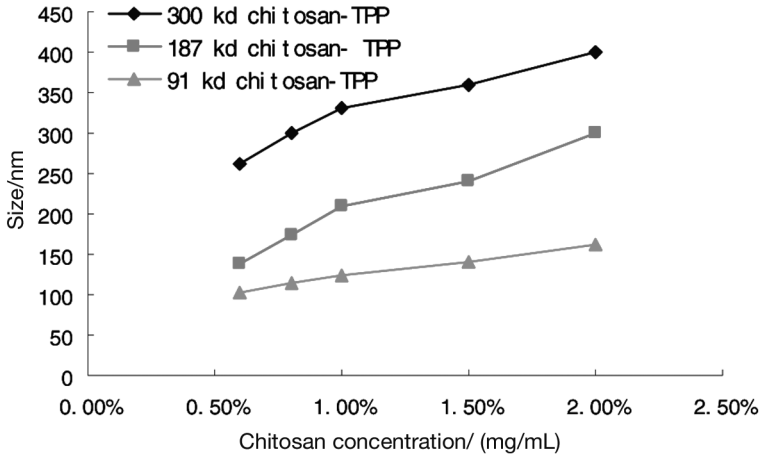

Fig. 2. Effect of chitosan concentration on size of chitosan particles.

Table 3
Effect of Chitosan Concentration on Size of Nanoparticles[a]

Chitosan concentration (%)	TPP concentration (mg/mL)						
	0.125	0.25	0.375	0.50	0.625	0.75	1.0
0.10	↓↓↓↓↓↓	↓↓↓↓↓↓	↓↓↓↓↓↓	↓↓↓↓↓↓	↓↓↓↓↓↓	↓↓↓↓↓↓	↓↓↓↓↓↓
0.30	↑↑↑↑↑↑	↓↓↓↓↓↓	↓↓↓↓↓↓	↓↓↓↓↓↓	↓↓↓↓↓↓	↓↓↓↓↓↓	↓↓↓↓↓↓
0.50	↑↑↑↑↑↑	↑↑°↑↑↑	↓↓↓↓↓↓	↓↓↓↓↓↓	↓↓↓↓↓↓	↓↓↓↓↓↓	↓↓↓↓↓↓
0.80	↑↑↑↑↑↑	↑↑°↑↑↑	°°°°°°	↓↓↓↓↓↓	↓↓↓↓↓↓	↓↓↓↓↓↓	↓↓↓↓↓↓
1.0	↑↑↑↑↑↑	↑↑°↑↑↑	°°°°°°	°°°°°°	↓↓↓↓↓↓	↓↓↓↓↓↓	↓↓↓↓↓↓
1.5	↑↑↑↑↑↑	↑↑°↑↑↑	°°°↑°°	°°°°°°	°°°°°°	↓↓↓°°↓	↓↓↓↓↓↓
2.0	↑↑↑↑↑↑	↑↑°↑↑↑	°°°↑°°	°°°°°°	°°°°°°	°↓↓°°↓	↓↓↓↓↓↓

[a]The symbol ↓ means that aggregates were formed in the solution, ↑ means that solution was formed in the solution, and ° means that opalescent suspension was formed in the solution. There were six symbols in the intersection between chitosan concentration and TPP concentration. The sequence symbol denoted that a different phenomenon occurred with a different chitosan. The sequence of chitosan was the molecular weight of chitosan (91,000, 187,000, and 3,000,000 kDa) and degree of deacetylation of chitosan (75, 85, and 97%), respectively.

Effect of Chitosan Concentration on Size of Chitosan Nanoparticles

The results in Table 3 show that the formation of nanoparticles was possible only within some moderate concentrations of chitosan and TPP. Some opalescent suspension was formed between TPP solution of 0.80–2.0 mg/mL and chitosan solution of 0.375–0.625 mg/mL. It has been previously reported that the highly viscous nature of the gelation medium hindered the encapsulation of drug in the study of chitosan microspheres *(26)*. Thus, it was supposed that a relatively lower viscosity of chitosan with a lower concentration promoted the formation of nanoparticles between chitosan and TPP.

Effect of pH on Size of Chitosan Nanoparticles

Chitosan nanoparticles were successfully prepared by ionic gelation method. Figure 3 presents the effects of pH on particle size. The mean diameter of chitosan nanoparticles decreased with an increase in pH, indicating an influence of pH on particle size. This could be related to different chitosan molecular conformation with changing pH before nanoparticle formation. Because the isoelectric point of chitosan was 6.8, the majority of amino groups were protonated to form an extended molecular chain in acid solution owing to strong repulsion existing among positively charged amino groups at low pH (3.0) *(27)*. A more extended spherical shape was formed on the addition of TPP solution. With an increase in pH (from 3.0 to 7.0), positive charges would be neutralized with gradual deprotonation of amino groups, resulting in a less extended molecular chain of chitosan to form uniform small nanoparticles.

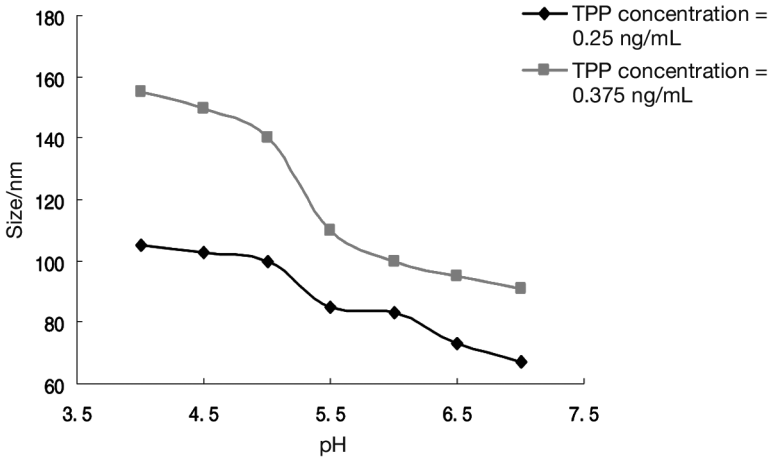

Fig. 3. Effect of pH on size of chitosan nanoparticles.

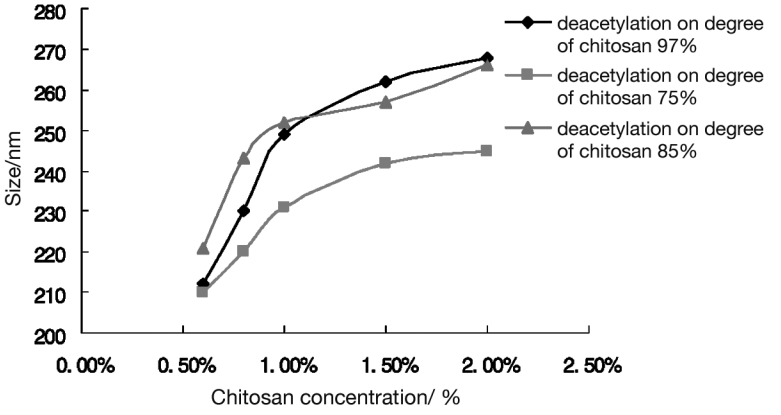

Fig. 4. Effect of degree of deacetylation of chitosan on size of nanoparticles.

Effect of Degree of Deacetylation on Size of Chitosan Nanoparticles

Figure 4 shows the influence of the degree of deacetylation on the size of nanoparticles. A gradual increase in particle size was noted with an increase in the degree of deacetylation. However, no significant change was observed. This trend might be explained by the fact that a higher-deacetylation-degree chitosan could interact with TPP more efficiently than a lower-deacetylation-degree chitosan could. This factor is outweighed by the fact that higher-deacetylation-degree chitosan was less soluble, and as a result, an increase in particle diameter or even aggregation might be obtained.

Effect of Stirring Rate Size of Chitosan nanoparticles

To study the effect of stirring rate on the size of chitosan nanoparticles, stirring rate was varied from 100 to 700 rpm; the results are shown in Fig. 5. It can be seen that the size of microspheres decreased with an increase

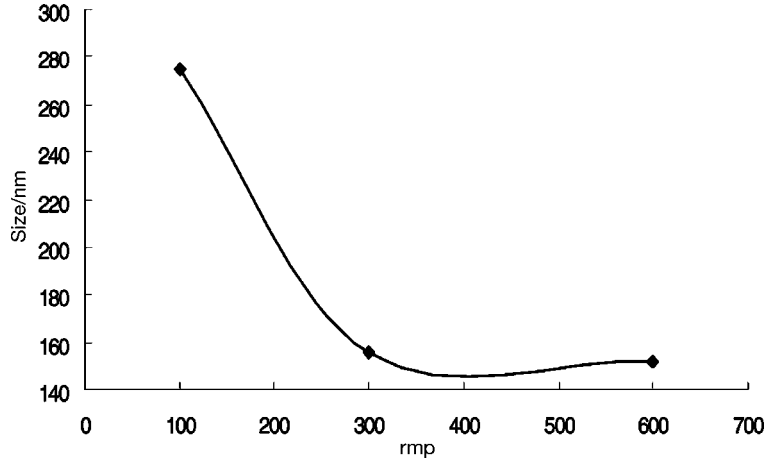

Fig. 5. Effect of stirring rate on size of chitosan nanoparticles.

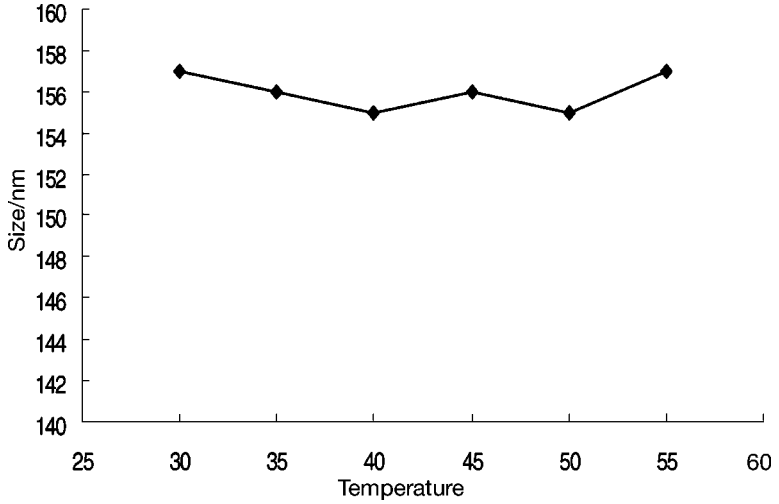

Fig. 6. Effect of temperature on size of chitosan nanoparticles.

in stirring rate. This trend could be explained by the energy transfer differences for different stirring rates. The results confirmed the findings of Xu and Du *(28)* and Janes et al. *(29)*.

Effect of Temperature on Size of Chitosan Nanoparticles

Figure 6 shows the effect of temperature on the size of chitosan nanoparticles. The size of chitosan nanoparticles almost did not change from 30 to 60°C. However, above 60°C, the solution became transparent, and chitosan nanoparticles were not fabricated. An explanation for this phenomenon is that the chitosan molecular chain might be cut short and fabrication was not done under the same conditions.

Table 4
Experimental Design and Results of FFD

Run	X_1	X_2	X_3	X_4	X_5	Size of nanoparticles (nm)
1	–1	–1	1	–1	–1	110
2	–1	1	1	1	1	132
3	1	–1	–1	1	1	98
4	–1	–1	1	1	–1	112
5	–1	1	1	–1	1	135
6	1	1	–1	–1	–1	120
7	1	1	1	–1	–1	115
8	1	1	–1	1	1	104
9	–1	–1	–1	–1	–1	70
10	–1	1	1	–1	–1	140
11	1	1	–1	–1	1	98
12	1	1	1	1	–1	168
13	1	–1	1	–1	1	125
14	–1	–1	–1	–1	1	70
15	–1	–1	–1	1	–1	70
16	1	–1	–1	–1	–1	100
17	1	–1	1	1	–1	126
18	–1	–1	–1	1	–1	110
19	–1	1	–1	1	1	110

Optimization of Factors for Size of Chitosan Nanoparticles

Five factors were set as two different variables, and a 2^{5-2} FFD was used to evaluate the approximate polynomial (first-order model) for all independent variables. The 2^{5-2} FFD required 19 experiments. Table 4 presents the experimental design and results of this design. The size of chitosan nanoparticles varied greatly, from 70 to 168 nm, in different experiments. The data were analyzed based on Eq. 4, and the model was given as follows:

$$Y = 109.20 + 3.30X_1 + 15.50X_2 + 19.70X_3 + 2.20X_4 - 6.50X_5 \quad (4)$$

Chitosan concentration, molecular weight of chitosan, stirring rate, and solution pH had positive effects on the size of chitosan nanoparticles at the tested levels, whereas temperature had negative effects. Table 4 and Fig. 7 give the results of regression analysis of the data obtained in Table 6. Chitosan concentration, solution pH, and molecular weight of chitosan were the most important factors affecting the size of chitosan nanoparticles at a probability of 95%, whereas temperature and stirring rate were not significant. The coefficient of determination, R^2, of the first-order model was calculated to be 0.9272 (Table 5). This indicated that only 7.28% of the total variation was not explained by the model. The statistical significance of the model, which was 35.67, was also confirmed by an F test. This value showed that the model adequately represented the data at a probability

Table 5
Results of FFD Regression Analysis for Size of Nanoparticles[a]

	Regression analysis for size of nanoparticles		
Term	Coefficient	*t* value	Significance level
Intercept	113.90	59.86	0.000
X_1	8.00	4.20	0.001
X_2	13.80	7.25	0.000
X_3	19.40	10.20	0.000
X_4	1.100	0.58	0.572
X_5	–3.700	–1.94	0.072

[a]$R^2 = 0.9272$; $R = 0.9012$.

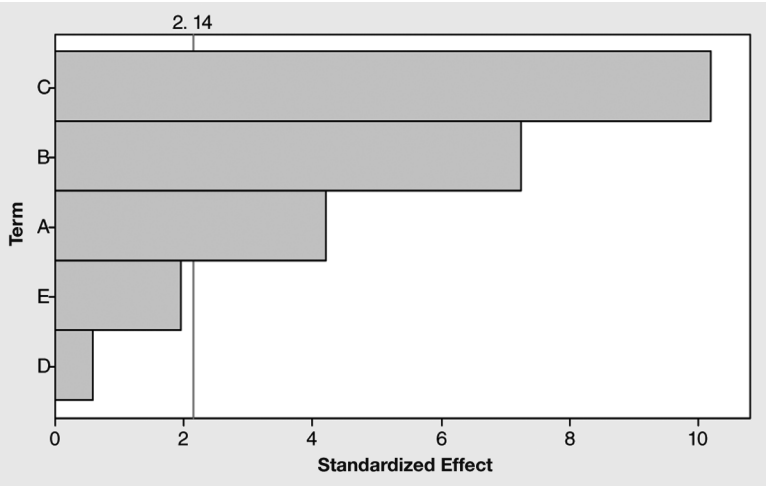

Fig. 7. Pareto chart of standardized effects.

Table 6
Analysis of Variance for Size of Nanoparticles

Source	Sum of squares	Degrees of freedom	Mean square	*F* value	Prob > F
Model	12,914	5	2582.80	35.67	0.000
Residual error	1014	14	72.41		
Corrected total	13,928	19	733.05		

level of 95%. Chitosan concentration, molecular weight of chitosan, and solution pH were chosen for further investigation in order to obtain optimal concentrations.

Based on the model equation obtained, experiments on the path of steepest ascent were conducted. New central points were reallocated and

Table 7
Experimental Design and Results of 2^3 CCD

Run	Chitosan concentration	TPP concentration	Solution pH	Size of nanoparticles (nm)	Predicted value
1	1	1	1	168	160.6
2	1	1	–1	76	82.7
3	1	–1	1	143	137.5
4	1	–1	–1	60	64.6
5	–1	1	1	152	146.3
6	–1	1	–1	70	74.3
7	–1	–1	–1	50	56.2
8	–1	–1	1	131	123.1
9	–1.682	0	0	90	90.9
10	1.682	0	0	110	110.0
11	0	–1.682	0	80	81.0
12	0	1.682	0	115	115.6
13	0	0	–1.682	70	56.4
14	0	0	1.682	163	178.2
15	0	0	0	100	100.5
16	0	0	0	102	100.5
17	0	0	0	101	100.5
18	0	0	0	100	100.5
19	0	0	0	100	100.5
20	0	0	0	100	100.5
21	0	0	0	101	100.5
22	0	0	0	100	100.5
23	0	0	0	100	100.5

Table 8
Results of Regression Analysis for Size of Chitosan Nanoparticles

	Regression analysis for size of chitosan nanoparticles		
Term	Coefficient	*t* value	Significance level (p)
X_1	5.685	2.919	0.0106
X_2	10.315	5.297	0.00009
X_3	36.205	18.59	0.00000
$X_1 \times X_1$	0.1181	0.06540	0.9487
$X_2 \times X_2$	–0.7658	0.4242	0.6775
$X_3 \times X_3$	5.9512	3.297	0.00489
$X_1 \times X_3$	1.500	0.5896	0.5643
$X_2 \times X_3$	1.250	0.4913	0.6303

the levels of three variables are given in Table 2. The second optimization was performed using a CCD. Tables 7–9 show the experimental design and results of analysis for 23 trials performed using the experimental designs.

Table 9
Analysis of Variance for Predictive Equation for Size of Chitosan Nanoparticles[a]

Source	Sum of squares	Degrees of freedom	Mean square	*F* value	Prob > *F*
Model	19,792.81997	3	6597.60666	94.33435	0.00000
Residual error	1328.83221	19	69.93854		
Corrected total	21,121.65217	22	960.07510		

[a] $R^2 = 0.937087$; $R = 0.968032$.

The corresponding second-order response model is given in Eq. 5 after DPS analysis for the regression:

$$Y = 100.42 + 5.685X_1 + 10.315X_2 + 36.205X_3 + 0.1181X_1 \times X_1 - 0.7658X_2 \times X_2 + 5.9512X_3 \times X_3 + 1.500X_1 \times X_3 + 1.250X_2 \times X_3 \quad (5)$$

The goodness of fit of the model was checked by the coefficient of determination, R^2, which was calculated to be 0.9371, indicating that 93.71% of the variability could be explained by the model (Table 8). This indicated that Eq. 5 was a suitable model to describe the size of chitosan nanoparticles. The Student *t* distribution and the corresponding *p* value, along with the parameters estimated, are given in Table 8. The *p* values were used to check the significance of the coefficients, which, in turn, were necessary to understand the pattern of the effect of different variables and their interactions. Table 8 reveals that the linear term of X_1, X_2, X_3; the quadratic coefficients (X_1^2, X_2^2, X_3^2); and the interaction between X_3 and X_2 (or X_1) had remarkable effects on the size of chitosan nanoparticles, suggesting that the effect of the second-order model was the main factor that affected the size from the linear term.

The response surfaces based on these coefficients are shown in Fig. 8 with one variable kept at the central level and the other two varying within the experimental range, showing the stationary ridge shape in surface plots. The optimum levels of the following three variables, which gave minimum response, were obtained from Eq. 5: chitosan concentration of 0.664%, TPP concentration 0.199 mg/L, and solution pH of 7.0. A minimum size of chitosan nanoparticles of 42 nm was predicted corresponding to the optimal levels of the three variables.

To confirm the predicted results of the model, experiments using optimal conditions were performed and a value of 42 ± 5 nm ($n = 4$) was obtained. The good correlation between two results verified the validity of the response model and the existence of an optimal point.

Conditions of Immobilization

Effect of Time on Immobilization

Neutral proteinase was immobilized on chitosan nanoparticles at different times. The residual protein of the solution was determined using the

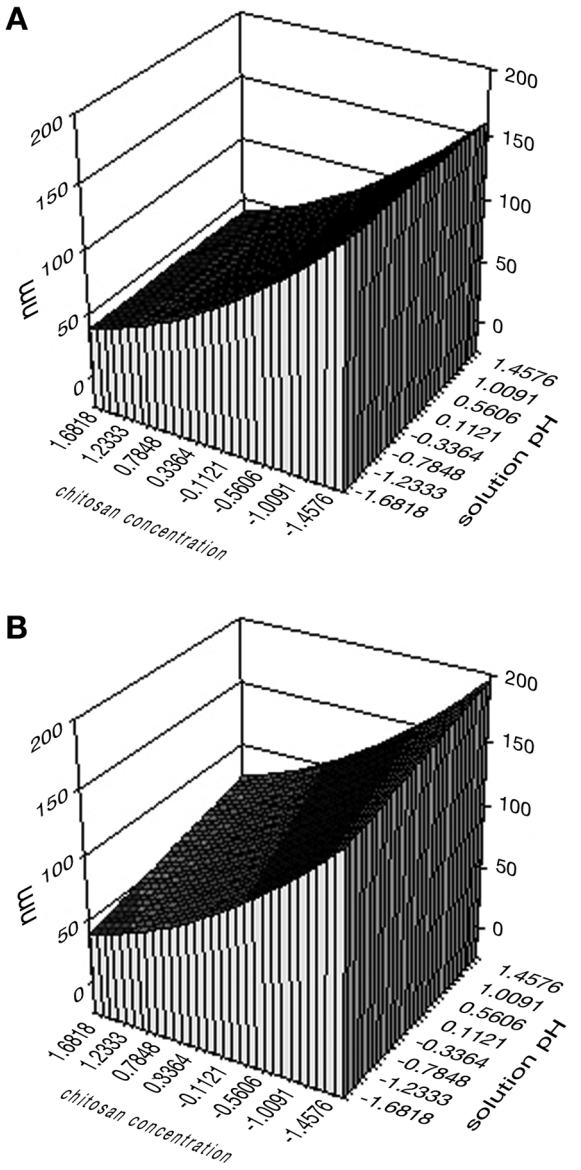

Fig. 8 Response surface graphs of size of chitosan nanoparticles affected by **(A)** chitosan concentration and solution pH and **(B)** TPP concentration and solution pH. The plot was obtained with the 2^3 factorial CCD and all of the variables were given in coded levels.

method described above. As shown in Fig. 9, the optimal immobilization time was 15 min. The relative immobilization rate increased with an increase in immobilization time. Higher relative immobilized rate (99.2%) and enzyme activity (1672.5 U/g) occurred on chitosan nanoparticles at an immobilization time of 15 min. When the immobilization time was >15 min, the relative immobilization rate did not increase any more. Li et al. *(30)*

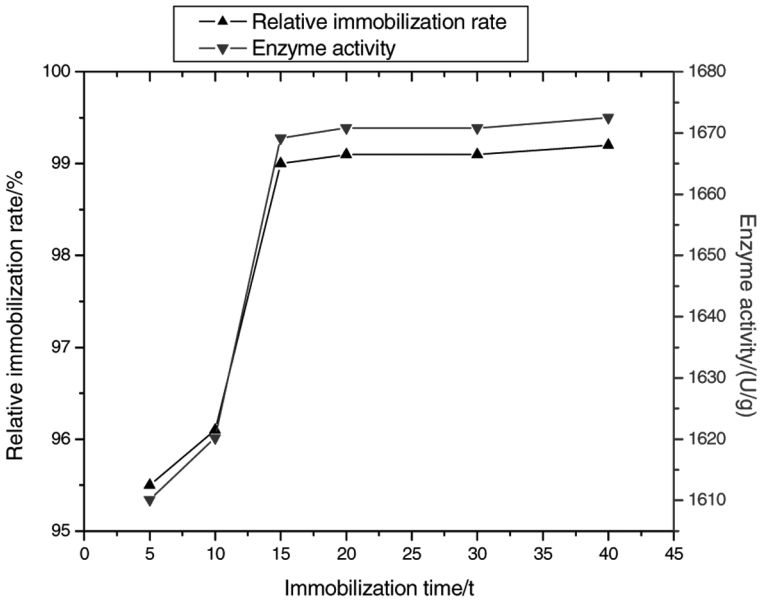

Fig. 9. Effect of immobilization time on immobilization rate.

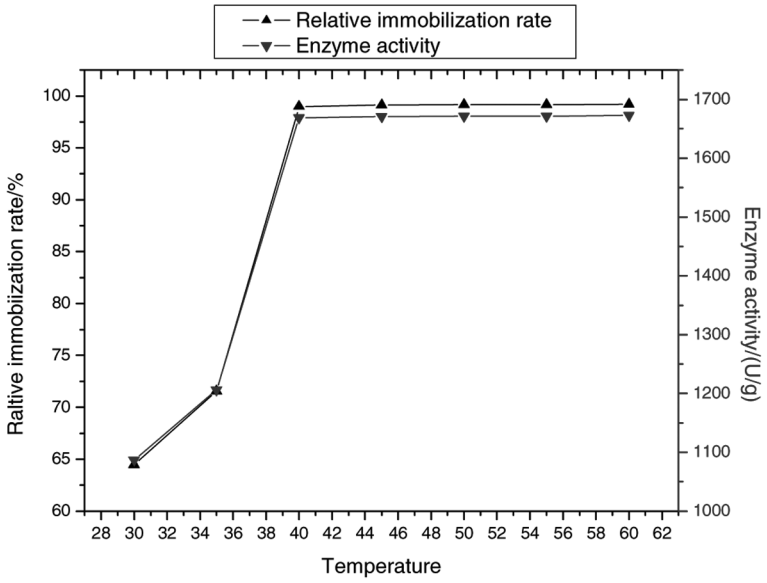

Fig. 10. Effect of immobilization temperature on enzyme immobilization.

investigated the immobilization condition of AS 1.398 neutral proteinase. The immobilization time was 8.0 h. Thus, the immobilization velocity with chitosan nanoparticles was very quick because of their larger specific surface area of contact.

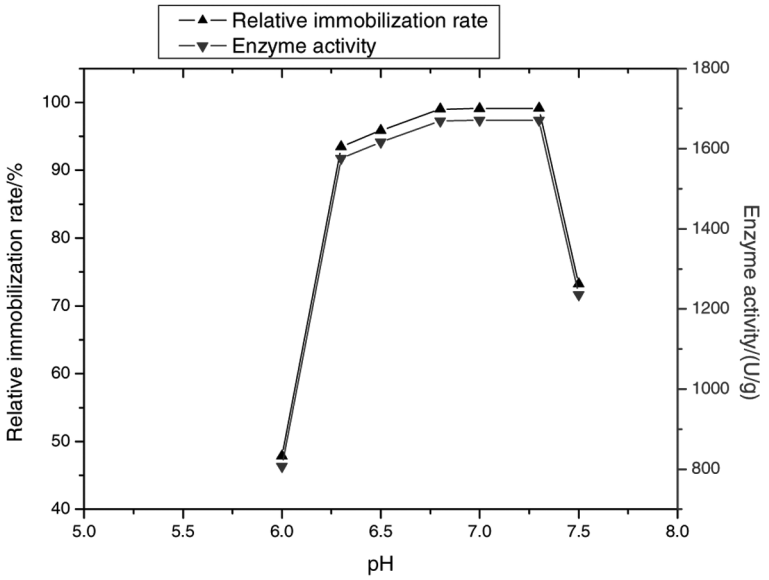

Fig. 11. Effect of pH on enzyme immobilization.

Effect of Temperature on Immobilization

The effect of temperature on the enzyme activity of immobilized enzyme and immobilized rate was also investigated. It was observed that the optimal immobilization temperature was 40°C. Figure 10 shows the enzyme activity and relative immobilized rate. A significant increase in enzyme activity was observed at 40°C. A maximum activity of 1672.5 U/g for neutral proteinase immobilized on chitosan nanoparticles was obtained at the optimum temperature. A higher immobilized rate of 99.2% was also achieved. This increment in the enzyme activity was in agreement with some possible mechanisms of immobilization of proteinase. Conventional immobilization, in the best case, could fully preserve the enzyme activity. On the basis of neutral proteinase structure, the hydrophilic areas surrounding the catalytic site might be exposed after immobilization of neutral proteinase. Chiou and Wu *(31)* studied the effect of reaction temperature on the enzyme activity of free and immobilized lipase. Maximum activities of 1.58 and 19.28 U/g of chitosan for lipase immobilized on dry and wet chitosan beads, respectively, were obtained at the optimal reaction conditions.

Effect of pH on Immobilization

Neutral proteinase was immobilized on chitosan nanoparticles at different pH values in phosphate buffer solutions. The residual protein of solution was determined as the method described above. As shown in Fig. 11, the optimal immobilization pH was 7.4. Relative immobilization rate increased with an increase in the pH of the solution. However, when the solution pH was greater than 6.3, the relative immobilization rate of

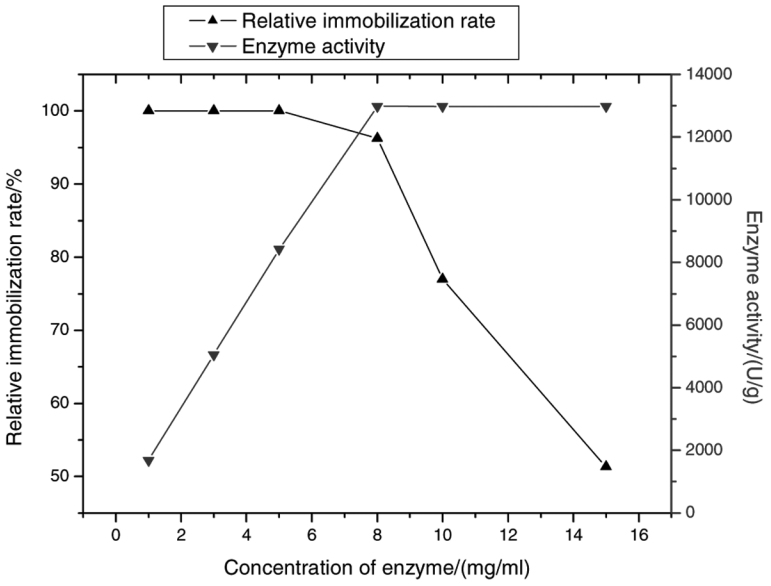

Fig. 12. Effect of amount of added enzyme on enzyme immobilization under optimal conditions.

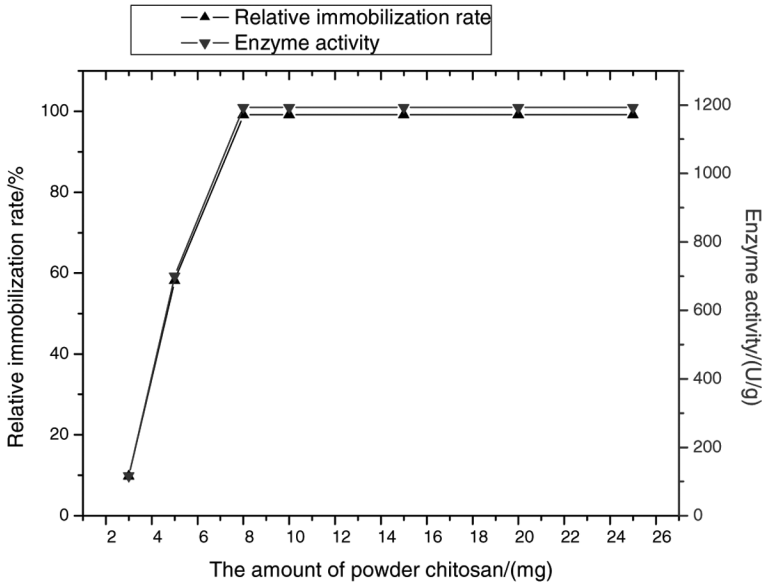

Fig. 13. Effect of chitosan powder on enzyme immobilization.

neutral proteinase increased slowly. When the solution pH was less than 7.4, the relative immobilization rate began to decrease. This might be why the chitosan nanoparticles began to assemble into larger chitosan microparticles.

Effect of Amount of Added Enzyme on Chitosan Nanoparticles

Under the optimal immobilization conditions, different amounts of neutral proteinase were immobilized on chitosan nanoparticles. As shown in Fig. 12, the optimal amount of protein was 8 mg/mL. An experiment to determine the immobilization rate of chitosan nanoparticles contrasted with chitosan powder was conducted; the results are presented in Fig. 13. Chitosan nanoparticles had a better immobilization rate than chitosan powder. Because chitosan nanoparticles had a larger specific surface area of contact, the efficiency of immobilization in terms of protein loading was larger compared with that of immobilization using chitosan powder. However, these results were found to be the opposite of those of Chiou and Wu *(31)*. They thought that dry chitosan beads had a smaller particle size, and that the efficiency of protein immobilization was less than that of immobilization using wet chitosan beads.

Conclusion

The formation of chitosan nanoparticles could be controlled simply by varying the key processing conditions of chitosan concentration, TPP concentration, and solution pH. Within the tested range of conditions, an increase in particle size showed a simple linear relationship to increasing TPP concentration. Solution pH and chitosan concentration also had a profound influence on the stability of the nanoparticle system.

Response surface methodology involving an experimental design and regression analysis was used to evaluate the effects of chitosan concentration, TPP concentration, solution pH, stirring rate, and temperature on the size of chitosan nanoparticles. Chitosan concentration, TPP concentration, and solution pH significantly affected the size of chitosan nanoparticles. The effect of temperature and stirring rate on the size of chitosan nanoparticles was not significant. A predictive model for the size of chitosan nanoparticles was established. The adequacy of the predictive model was verified effectively by the validation data.

Chitosan nanoparticles prepared by ionization gelation method were spherically shaped, and their mean particle size was less than 50 nm. Neutral proteinase could be immobilized on the surface of chitosan nanoparticles. The optimal immobilization conditions for neutral proteinase were 1.0 mL of 1.0 mg/mL neutral proteinase in phosphate buffer (0.020 mol/L, pH 7.4) reacted with 8.0 mL of chitosan nanoparticle solution at 40°C for 15 min. Under the immobilization conditions, the enzyme activity yield was 84.3%, and catalytic capability was calculated to be 1686 U/mg of support.

References

1. Juang, R. S., Wu, F. C., and Tseng, R. L. (2001), *Bioresour. Technol*. **80,** 187–193.
2. Monteiro, O. A., Jr. and Airoldi, C. (1999), *Int. J. Biol. Macromol.* **26,** 119–128.
3. Denkbas, E. B., Kilicay, E., Birlikseven, C., and Ozturk, E. (2002), *React. Funct. Polym.* **50,** 225–232.

4. Selmer-Olsen, E., Ratnaweera, H. C., and Pehrson, R. (1996), *Water Sci. Technol.* **34,** 33–40.
5. Kucera, J. (2004), *J. Chromatogr. B* **808,** 69–73.
6. Chiou, S. H. and Wu, W. T. (2004), *Biomaterials* **25,** 197–204.
7. Mi, F. L., Kuan, C. Y., Shyu, S. S., Lee, S. T., and Chang, S. F. (2000), *Carbohydr. Polym.* **41,** 389–396.
8. Berthold, A., Cremer, K., and Kreuter, J. (1996), *J. Control. Release* **39,** 17–25.
9. Tian, X. X. and Groves, M. J. (1999), *J. Pharm. Pharmacol.* **51,** 151–157.
10. Cui, Z. and Mumper, R. J. (2001), *J. Control. Release* **75,** 409–419.
11. Ohya, Y., Shiratani, M., Kobayashi, H., et al. (1994), *Pure Appl. Chem.* **31,** 629–642.
12. Bodmeier, R., Chen, H. G., and Paeratakul, O. (1989), *Pharm. Res.* **6,** 413–417.
13. Janes, K. A., Fresneau, M. P., Marazuela, A., et al. (2001), *J. Control. Release* **73,** 255–267.
14. Calvo, P., Remunan Lopez, C., Vila-Jato, J. L., et al. (1997), *J. Appl. Polym. Sci.* **63,** 125–132.
15. De Campos, A. M., Sanchez, A., and Alonso, M. J. (2001), *Int. J. Pharm.* **224,** 159–168.
16. Tokumisu, H., Hiratsuka, J., Sakurai, Y., et al. (2000), *Cancer Lett.* **150,** 177–182.
17. Shikata, F., Tokumitsu, H., Ichikawa, H., et al. (2002), *Eur. J. Pharm. Biopharm.* **53,** 57–63.
18. Fujimoto, M., Kunniaka, A., and Yoshino, H. (1974), *Agric. Biol. Chem.* **38,** 777–783.
19. Montgomery, D. C. (1991), *Design and Analysis of Experiments,* 3rd ed., John Wiley & Sons, New York.
20. Leong, Y. S. and Candau, F. (1982), *J. Phys. Chem.* **86,** 2269–2271.
21. Polk, A., Amsden, B., Yao, K. D., Peng, T., and Goosen, M. F. A. (1994), *J. Pharm. Sci.* **83,** 178–185.
22. Liu, L. S., Liu, S. Q., Ng, S. Y., Froix, M., Ohno, T., and Heller, J. (1997), *J. Control. Release* **43,** 65–74.
23. Kawashima, Y., Handa, T., Takenaka, H., Lin, S. Y., and Ando, Y. (1985), *J. Pharm. Sci.* **74,** 264–268.
24. Kawashima, Y., Handa, T., Kasai, A., Takenaka, H., and Lin, S. Y. (1985), *Chem. Pharm. Bull.* **33,** 2469–2474.
25. Gan, Q., Wang, T., Colette, C., et al. (2005), *Colloids Surf. B: Biointerfaces* **44,** 65–73.
26. Vandenberg, G. W., Drolet, C., Scott, S. L., and Noüe, J. D. (2001), *J. Control. Release* **77,** 297–307.
27. Kumar, M. N. V. R. (2000), *J. Pharm. Pharm. Sci.* **3,** 234–258.
28. Xu, Y. and Du, Y. (2003), *Int. J. Pharm.* **250,** 215–226.
29. Janes, K. A., Calvo, P., and Aloso, M. J. (2001), *Adv. Drug Deliv. Rev.* **47,** 83–97.
30. Li, T. M., Xu, X. L., Li, W., et al. (1998), *Pharm. Biotechnol.* **5,** 214–218.
31. Chiou, S. H. and Wu, W. T. (2004), *Biomaterials* **25,** 197–204.